Climate Dynamics (1998) 14:853–869

M. Wild · A. Ohmura · H. Gilgen · E. Roeckner
M. Giorgetta · J.-J. Morcrette

The disposition of radiative energy in the global climate system: GCM-calculated versus observational estimates

Received: 26 February 1998 / Accepted: 18 May 1998

Abstract A comprehensive dataset of direct observations is used to assess the representation of surface and atmospheric radiation budgets in general circulation models (GCMs). Based on combined measurements of surface and collocated top-of-the-atmosphere fluxes at more than 700 sites, a lack of absorption of solar radiation within the atmosphere is identified in the ECHAM3 GCM, indicating that the shortwave atmospheric absorption calculated in the current generation of GCMs, typically between 60 and 70 Wm^{-2}, is too low by 10–20 Wm^{-2}. The surface and atmospheric radiation budgets of a new version of the Max-Planck Institute GCM, the ECHAM4, differ considerably from other GCMs in both short- and longwave ranges. The amount of solar radiation absorbed in the atmosphere (90 Wm^{-2}) is substantially larger than typically found in current GCMs, resulting in a lower absorption at the surface (147 Wm^{-2}). It is shown that this revised disposition of solar energy within the climate system generally reduces the biases compared to the observational estimates of surface and atmospheric absorption. The enhanced shortwave absorption in the ECHAM4 atmosphere is due to an increase in both simulated clear-sky and cloud absorption compared to ECHAM3. The increased absorption in the cloud-free atmosphere is related to an enhanced absorption of water vapor, and is supported in stand-alone comparisons of the radiation scheme with synchronous observations. The increased cloud absorption, on the other hand, is shown to be predominantly spurious due to the coarse spectral resolution of the ECHAM4 radiation code, thus providing no physical explanation for the "anomalous cloud absorption" phenomenon. Quantitatively, however, an additional increase of atmospheric absorption due to clouds as in ECHAM4 is, at least at low latitudes, not in conflict with the observational estimates, though this does not rule out the possibility that other effects, such as highly absorbing aerosols, could equally contribute to close the gap between models and observations. At higher latitudes, however, the increased cloud absorption is not supported by the observational dataset. Overall, this study points out that not only the clouds, but also the cloud-free atmosphere might be responsible for the discrepancies between observational and simulated estimates of shortwave atmospheric absorption. The smaller absorption of solar radiation at the surface in ECHAM4 is compensated by an increased downward longwave flux (344 Wm^{-2}), which is larger than in other GCMs. The enhanced downward longwave flux is supported by surface measurements and by a stand-alone validation of the radiation scheme for clear-sky conditions. The enhanced flux also ensures that a sufficient amount of energy is available at the surface to maintain a realistic intensity of the global hydrological cycle. In contrast, a one-handed revision of only the shortwave radiation budget to account for the increased shortwave absorption in GCM atmospheres may induce a global hydrological cycle that is too weak.

M. Wild (✉) · A. Ohmura · H. Gilgen
Swiss Federal Institute of Technology, Department of Geography, Winterthurerstr.190, CH-8057 Zürich, Switzerland
E-mail: wild@geo.umnw.ethz.ch

E. Roeckner · M. Giorgetta
Max-Planck Institute for Meteorology, Bundesstr. 55, D-20146 Hamburg, Germany

J.-J. Morcrette
ECMWF, Shinfied Park, Reading, Berkshire, RG2 9AX, UK

1 Introduction

The radiation budget of the Earth is fundamental for the understanding of the genesis and evolution of the global climate system. Due to recent advances in spaceborne measurements, the net solar energy absorbed by the global climate system is accurately known (Barkstrom et al. 1990). However, the partitioning of the

absorbed energy between the atmosphere and the Earth's surface is not as well known, due to a lack of adequate observations. This uncertainty is reflected in the current generation of general circulation models (GCMs), which show substantial differences in these fundamental quantities (e.g., Gutowski et al. 1991; Randall et al. 1992; Wild et al. 1995a; Garratt and Prata 1996; Li et al. 1997).

More insight into this problem can now be gained through the availability of a new comprehensive database of the worldwide measured surface energy fluxes compiled at the Swiss Federal Institute of Technology, the Global Energy Balance Archive (GEBA) (Gilgen et al. 1997). Making extensive use of GEBA, Wild et al. (1995a) concluded that current GCMs typically overestimate the absorption of solar radiation at the surface when compared to more than 700 surface observation sites. Similar results were obtained in the works of Garratt (1994) and Arking (1996), who used subsets of an earlier GEBA version, including 93 and 173 observation sites, respectively. Wild et al. (1995a) ascribed the overestimation of surface insolation to an underestimation of the absorption of solar radiation in the GCM atmosphere, based on considerations of global mean surface and top-of-the-atmosphere (TOA) budgets. The present study investigates this argument more thoroughly by combining the comprehensive set of surface observations used in Wild et al. (1995a) with collocated satellite observations. This allows an estimate of the absorption of solar radiation within the atmospheric columns above the 720 sites chosen for this study from GEBA. This dataset is applied to two GCMs from the Max Planck model series, ECHAM3 and ECHAM4. While the earlier version, ECHAM3, calculates surface and atmospheric radiation budgets typical for the current generation of GCMs, ECHAM4 calculates considerably lower values of absorbed solar radiation at the surface due to an enhanced absorption of solar radiation within the atmosphere.

An underestimated absorption of solar radiation in the atmosphere may be attributed to a lack of absorption either in clouds or in the cloud-free atmosphere. Recently, evidence has been presented that the GCM-calculated absorption of solar radiation by clouds may be underestimated (Cess et al. 1995; Ramanathan et al. 1995). Moreover, Wild et al. (1995a), Barker and Li (1995), and Arking (1996) presented evidence that the GCM-calculated absorption of solar radiation in the cloud-free atmosphere is underestimated. In ECHAM4, both clear-sky and cloud absorption are enhanced compared to other GCMs. The present study investigates the compatibility of these changes with the observational dataset, along with a critical discussion of the origins of the enhanced absorption.

The longwave (thermal) radiation emitted into space by the climate system to balance the net solar absorption is also well established through satellite measurements (Barkstrom et al. 1990). The longwave exchange between the earth's surface and the atmosphere, however, is known to a lesser degree. In particular, the downwelling atmospheric emission towards the surface (downward or incoming longwave radiation) is only poorly known on the global scale. Accordingly, considerable differences exist in the simulated downward longwave fluxes between GCMs (Wild et al. 1995a). Based on observations from GEBA, Wild et al. (1995a) presented evidence that the downward longwave radiation at the Earth's surface is underestimated in ECHAM3 and other GCMs. These findings were supported in the study of Garratt and Prata (1996). Apart from the GCMs, a general trend towards underestimation of the downward longwave radiation by previous works in radiation climatology was suggested by Ohmura and Gilgen (1992). The global mean downward longwave radiation in ECHAM4 is larger than in ECHAM3 and other GCMs, thereby compensating for the smaller amount of solar energy available at the surface. Thus, the assessment of the revised partitioning between the shortwave and longwave contribution to the surface net radiation is a further focus of this study, using the information contained in the surface observations.

2 Models

As previously noted, the focus in the present study is on the third and fourth generation versions of the ECHAM GCM, namely ECHAM3 and ECHAM4, developed at the Max Planck Institute for Meteorology, Hamburg. Additionally, global radiation budgets from a number of other GCMs have been collected from the literature and through personal communication.

The ECHAM3 GCM is described in detail in Roeckner et al. (1992). This GCM evolved from the spectral numerical weather forecasting model of the European Centre for Medium Range Weather Forecasts (ECMWF) and has been extensively modified in Hamburg for climate applications. These modifications include inter alia an additional prognostic equation for cloud water and the radiation scheme of Hense et al. (1982). This radiation scheme is based on a two-stream approximation described by Kerschgens et al. (1978) and Zdunkowski et al. (1980) with the delta-Eddington approximation for clouds. The longwave spectrum is divided into six spectral intervals which take into account absorption due to water vapor, carbon dioxide, ozone and aerosols. An inversion procedure is employed to define the relevant optical properties by matching the two-stream solutions to more accurate model solutions obtained by a line-by-line model (Hense et al. 1982), based on spectroscopic data of LOWTRAN3 (Selby and McClatchey 1975). For cloud droplet absorption, an emissivity formulation is used (Stephens 1978). Scattering of longwave radiation is neglected. The shortwave spectrum is divided into four intervals ranging from 0.215 μm–3.58 μm, with the same gaseous absorbers as previously mentioned (Table 1). The optical thickness for gas absorption is a function of the effective absorber amount and is determined similarly to the longwave part. Rayleigh scattering is included via a parametric expression of optical thickness. Scattering and absorption coefficients of stratospheric, urban, and maritime aerosols are taken from a dataset provided by Shettle and Fenn (1976). Cloud optical depth and single scattering albedo are derived from the cloud water path (Stephens 1978).

The ECHAM4 incorporates revisions of a number of key climatic processes, as described in Roeckner et al. (1996). One of the most fundamental changes between the ECHAM3 and ECHAM4 models

Table 1 Spectral intervals and absorbers in the solar part of the ECHAM3 (Hense et al. 1982) and ECHAM4 (Morcrette 1991) radiation schemes

Model	Spectral interval (μm)	Absorber
ECHAM3	0.215–0.685	O_3
	0.685–0.891	H_2O
	0.891–1.273	H_2O
	1.273–3.580	H_2O, CO_2
ECHAM4	0.25–0.68	O_3
	0.68–4.0	H_2O, CO_2

is the inclusion of a completely new radiation code. This code is based on the scheme developed by Morcrette (1991) for the numerical weather prediction model, cycle 44, of the ECMWF. This scheme uses a two-stream method based on Fouquart and Bonnel (1980) for the solar part and Morcrette et al. (1986) for the longwave part. The solar spectrum is divided into two bands (Table 1). Coefficients for the gaseous absorption are calculated from the 1991 version of the Air Force Geophysics Laboratory (AFGL) line parameters compilation (Rothman et al. 1992). Rayleigh scattering is included via a parametric expression of optical thickness. As in ECHAM3, aerosol scattering and absorption coefficients are based on Shettle and Fenn (1976). The shortwave cloud radiative properties are a function not only of the cloud water path as in ECHAM3, but also of the effective radius of the cloud particles. The longwave spectrum is divided into six bands with gas absorption coefficients fitted from AFGL. The water vapor continuum parametrization is based on Roberts et al. (1976). As in ECHAM3, clouds are treated as gray bodies with a longwave emissivity depending on the cloud water path (Stephens 1978).

The ECMWF code has undergone a number of changes at MPI. Additional greenhouse gases such as methane, nitrous oxide, 16 CFCs, and the 14.6 μm band of ozone have been considered as well as various types of aerosols (R. v. Dorland personal communication). Moreover, the water vapor continuum has been revised to include temperature-weighted band averages of *e*-type absorption, and a band dependent ratio of (*p*–*e*)-type to *e*-type continuum absorption (Giorgetta and Wild 1995). The single scattering properties of cloud droplets and ice crystals are determined on the basis of high-resolution Mie calculations with subsequent averaging over the relatively wide spectral range of the GCM weighted by the Planck function (Rockel et al. 1991). This procedure has been applied for different effective radii, and polynomial fits are finally employed which allow the expression of the single scattering parameters as analytical functions of the effective radius within the respective spectral domain. Since the effective radii are parametrized in terms of the simulated liquid and ice water content, respectively, the cloud optical properties are basically determined by the model itself (Roeckner et al. 1996).

3 Experiments

This study is based on simulations performed with ECHAM3 and ECHAM4 using present-day boundary conditions ("control runs"). In these experiments, sea-surface temperatures and sea-ice were prescribed daily by linear interpolation between mean monthly climatologies from the AMIP SST and sea-ice dataset (Gates 1992) representative of the period 1979–1988.

The simulations have been performed using different horizontal resolutions up to wave number T106 (1.1° gridspacing). The ECHAM3 and ECHAM4 high resolution (T106) simulations were integrated for 5 and 10 y, respectively, at the Swiss Scientific Computing Center (CSCS), in a joint project between the Max Planck Institute for Meteorology, Hamburg, and the Swiss Federal Institute of Technology, Zurich. Multidecadal integrations at lower resolutions (T21, T42), using the same experiment type, have been performed at the Max Planck Institute with both models.

Wild et al. (1995a) showed that the horizontal resolution has no significant effect on the global and zonal mean surface irradiances in ECHAM3 simulations ranging from T21 to T106. The surface, atmospheric and TOA radiation budgets of ECHAM3 and ECHAM4 were also found to vary insignificantly with horizontal resolution on global and zonal scales. Therefore, the conclusions presented in this study do not critically depend on the horizontal resolution of the models. The results shown are generally based on the T42 simulations, where additional clear-sky diagnostics were available.

4 Observational data

The present study is entirely based on direct measurements of radiative fluxes. Semi-empirical estimates are not used. The surface flux climatologies are retrieved from a database containing the worldwide instrumentally measured surface energy fluxes, the Global Energy Balance Archive (Gilgen et al. 1997). This database currently contains 220 000 monthly mean fluxes for approximately 1600 sites, and has been used in a number of studies to assess GCM and satellite derived estimates of surface energy fluxes (e.g., Garratt 1994; Li et al. 1995a; Wild et al. 1995a, 1995b, 1996, 1997, Rossow and Zhang 1995; Garratt and Prata 1996). Gilgen et al. (1998) estimated the relative random error (root mean square error/mean) of the incoming shortwave radiation values in the GEBA at 5% for the monthly means and 2% for yearly means. The representativity of point measurements for a larger area is limited by temporal trends and local station effects (differences in the climatologies between stations in the same gridbox). Trends are negligible because the model integration period falls into the observation period at most sites and trends are generally small. The station effects have been estimated at approximately 5% of the station climatologies in 2.5°gridboxes (Gilgen et al. 1998). The large number of stations together with the interpolation procedure used in this study (see Sect. 5) ensure a representative assessment of the GCM fluxes with GEBA data (Wild 1997).

Error estimates for the longwave fluxes will be available in the near future from a longterm instrument comparison experiment jointly performed by the author's institute and the Swiss meteorological institute. The current best estimate is 5%.

The satellite climatologies of the radiative fluxes at the TOA, which are collocated with the observation stations at the surface, are ensemble averages from the Earth Radiation Budget Experiment (ERBE, Barkstrom et al. 1990) over the period 1985–1989, with a resolution of $2.5° \times 2.5°$. The uncertainties in the monthly averaged scanner data are estimated to within $\pm 5\ \mathrm{Wm}^{-2}$.

For the assessment of the radiation scheme in standalone mode, selected surface radiation measurements of

high quality and high temporal resolution are used together with upper air soundings from the aerological station at Payerne in Switzerland. Payerne is one of 14 presently active stations in the Baseline Surface Radiation Network (BSRN) of the World Climate Research Program (Ohmura et al. 1998).

5 Shortwave radiation

The global mean absorbed shortwave radiation at the Earth's surface calculated by ECHAM3, ECHAM4 and a number of other GCMs collected from the literature and personal communication is displayed in Fig. 1. Large differences of more than 30 Wm^{-2} can be seen in the global mean values among the various GCMs.

Wild et al. (1995a) demonstrated that the incoming shortwave radiation at the surface in the ECHAM3 GCM is substantially overestimated compared to a comprehensive dataset of surface observations. Based on considerations of global mean values, it was suggested that the overestimation of the surface fluxes is due to a lack of shortwave absorption within the atmosphere. This argument is further expanded in this section, using additionally collocated satellite observations of the TOA radiative fluxes above the sites where surface observations are available. Combining the flux measurements at the surface and at the TOA allows a direct estimate of the shortwave absorption in the atmospheric column above the observation sites. This dataset is applied to the radiation budgets of ECHAM3 and ECHAM4 in the following. For this purpose, the gridded model and ERBE data are interpolated to the 720 GEBA sites used in Wild et al. (1995a) by taking into account the four surrounding gridpoints weighted by their inverse spherical distance. The global distribution of these sites is shown in Fig. 1 of Wild et al. (1995a).

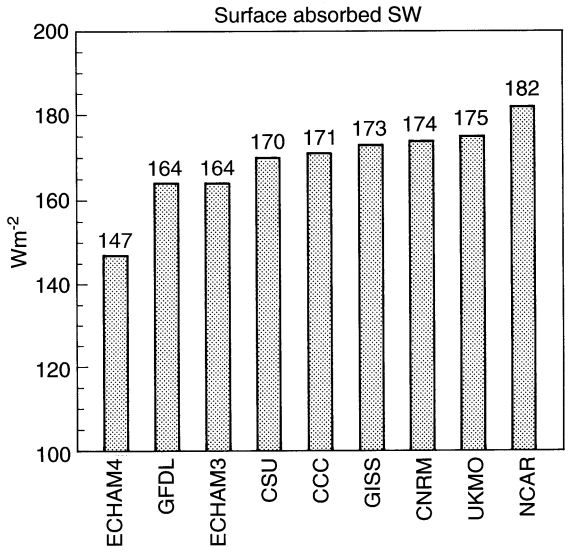

Fig. 1 Global annual mean absorbed shortwave radiation at the surface in various GCMs. *NCAR*, *GFDL*, *GISS* values from Gutowski et al. (1991), *CCC* value from Boer (1993), *CNRM* value from M. Déqué (personal communication, based on the ARPEGE model), *UKMO* value from R. Stratton (personal communication, based on model version HadAM2b), *CSU* value from Li et al. (1997). Units Wm^{-2}

5.1 Absorption at the TOA, in the atmosphere and at the surface

To assess the ability of ECHAM3 to capture the net (total) absorbed solar energy in the surface-atmosphere system at the GEBA locations, differences between the calculated annual mean net shortwave fluxes at the TOA and the ERBE fluxes have been determined (Fig. 2a). The agreement is within 20 Wm^{-2} at most sites. Globally, the model-calculated total absorbed shortwave energy of 235 Wm^{-2} is within the measurement uncertainty of the ERBE value of 237 Wm^{-2} (Barkstrom et al. 1990). This close agreement of the global mean values is partly the result of a tuning in the cloud scheme to match the global mean planetary albedo with the satellite estimate. The global mean surface and TOA radiation budgets of ECHAM3 and ECHAM4 are summarized in Table 2.

The ECHAM3-calculated incoming shortwave radiation at the surface has been compared with the GEBA sites in Wild et al. (1995a). To obtain a reference dataset for the absorbed shortwave radiation rather than the incoming shortwave radiation at the surface, the observed values of the incoming shortwave radiation have been combined with the collocated values of the surface albedo climatology used in ECHAM3 (Geleyn and Preuss 1983). Differences between the observation-based and ECHAM3-calculated surface shortwave absorption at the GEBA sites are presented in Fig. 2c. These differences show the errors in the ECHAM3-calculated shortwave surface absorption induced by shortcomings in the simulated incoming shortwave radiation. Possible errors due to deficiencies in the model surface albedo are thereby neglected. The likely range of the albedo error, however, cannot explain the large magnitude of the differences in Fig. 2c. Replacing the Geleyn and Preuss (1983) surface albedo climatology by two other, more recently established climatologies (Darnell et al. 1992; Claussen et al. 1994) had no significant impact on the calculated differences. These differences suggest a substantial model-overestimation of the absorbed shortwave radiation in the low latitudes and a slight underestimation at higher latitudes, as noted in Wild et al. (1995a) for the incoming shortwave radiation at the surface.

Differences in atmospheric absorption are determined as residuals of the net flux differences at the TOA

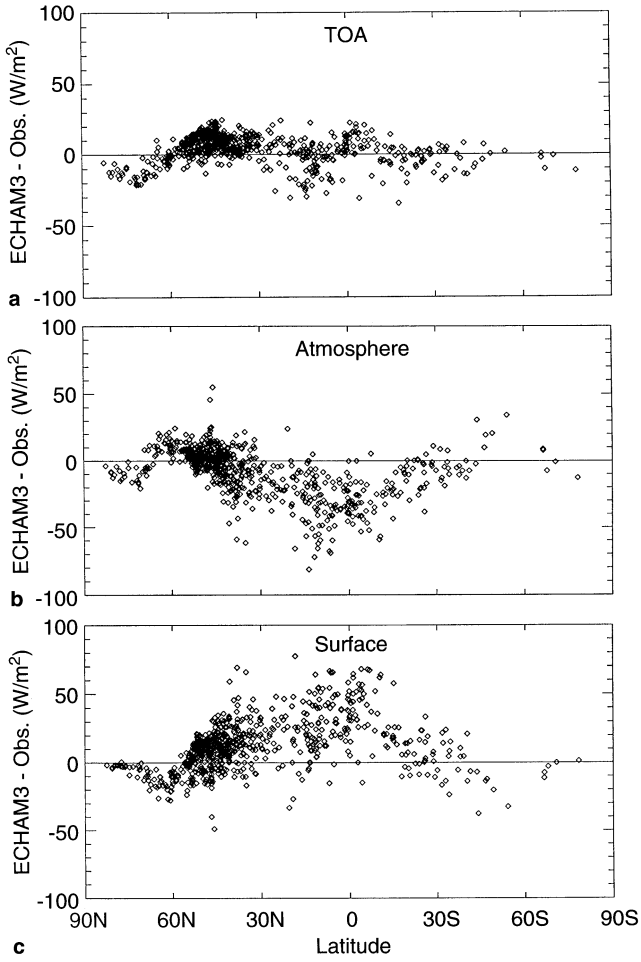

Fig. 2 **a** Difference between ECHAM3-calculated and observed annual net shortwave fluxes at the top-of-atmosphere above 720 GEBA sites as a function of the sites' latitudes. Observations from ERBE. **b** Differences in ECHAM3-calculated and observed annual atmospheric shortwave absorption at the GEBA sites derived from differences in net TOA and surface fluxes as a function of the sites' latitudes. **c** Difference between ECHAM3-calculated and observed annual net shortwave fluxes at the surface as a function of the sites' latitudes. Observations from GEBA. Units Wm^{-2}

Table 2 Global mean values of surface, atmospheric and TOA radiation budgets in ECHAM3 and ECHAM4. Units Wm^{-2}

	ECHAM3	ECHAM4
Top of atmosphere (Wm^{-2}):		
SW absorbed all-sky	235	237
SW absorbed clear-sky	284	286
SW cloud radiative forcing	− 49	− 49
LW emitted all-sky	− 233	− 235
LW emitted clear-sky	− 262	− 263
LW cloud radiative forcing	29	28
Atmosphere (Wm^{-2}):		
SW absorbed all-sky	71	90
SW absorbed clear-sky	63	72
SW cloud radiative forcing	8	18
Surface (Wm^{-2}):		
SW downward all-sky	189	170
SW absorbed all-sky	164	147
SW absorbed clear-sky	222	214
SW cloud radiative forcing	− 58	− 67
LW downward all-sky	334	344
LW downward clear-sky	311	323
LW upward	397	397
Net LW all-sky	− 63	− 53
LW cloud radiative forcing	− 23	− 21
Surface net radiation	101	94

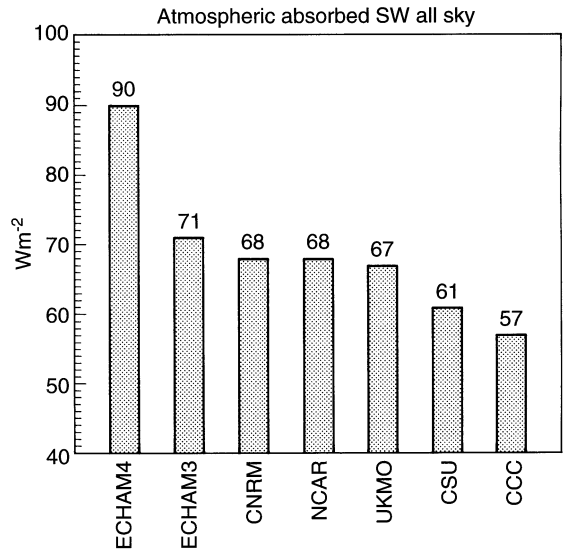

Fig. 3 Global annual mean absorbed shortwave radiation in the atmosphere ("all sky") in various GCMs. *CNRM* value from M. Déqué (personal communication, based on the ARPEGE model), *UKMO* value from R. Stratton (personal communication, based on model version HadAM2b), *NCAR*, *CSU*, *CCC* values from Li et al. (1997). Units Wm^{-2}

and at the surface (Fig. 2b). Figure 2b strongly suggests that the biases in the ECHAM3-calculated fluxes at the surface are predominantly due to biases in the atmospheric absorption rather than to biases in the net solar fluxes at the TOA. Thus, it is not so much a problem of calculating the correct total amount of solar energy absorbed by the climate system but rather one of partitioning the energy absorbed in the atmosphere and at the surface. Figure 2b indicates that the ECHAM3 shortwave atmospheric absorption is underestimated on the global scale, taking into account the fact that half of the Earth's surface is located between 30 °N and 30 °S, where the underestimation is largest. This suggests that the global mean shortwave atmospheric absorption of 71 Wm^{-2}, calculated in ECHAM3, is too small. This value can be seen compared with the ones of ECHAM4 and a number of other GCMs in Fig. 3. Apart from ECHAM4, these models show an even smaller atmospheric absorption than ECHAM3. This suggests that the underestimation of atmospheric absorption is a common problem in many current GCMs.

These results confirm the supposition of a lack of shortwave absorption in GCM atmospheres as stated in Wild et al. (1995a), and are in line with similar conclusions of Barker and Li (1995) and Li et al. (1997) based on satellite-derived references, and Arking (1996) based on a smaller set of surface observations.

It is also apparent from Fig. 3 that ECHAM4 calculates a substantially larger atmospheric absorption (90 Wm^{-2}) than the above mentioned models. A zonal comparison of the ECHAM3 and ECHAM4 shortwave radiation budgets at the TOA, in the atmosphere and at the surface is given in Fig. 4. While the TOA radiation budget, i.e., the total amount of solar energy absorbed by the global climate system, is very similar in ECHAM3 and ECHAM4, the partitioning of the solar absorption between the surface and atmosphere differs substantially between the two models. It is therefore interesting at this point to also evaluate the ECHAM4 radiation budget using the same reference dataset.

Differences between the annual mean ECHAM4-calculated net shortwave fluxes at the TOA and the ERBE fluxes have been determined in Fig. 5a for the 720 locations. The differences are of similar magnitude as in ECHAM3 (Fig. 2a), with errors less than 20 Wm^{-2}. This is in line with Table 2 and Fig. 4, which showed that net shortwave fluxes at the TOA in ECHAM3 and ECHAM4 do not differ greatly in the global and zonal mean. Further, global mean values of shortwave cloud radiative forcing and associated shortwave all-sky and clear-sky fluxes at the TOA do not change significantly in ECHAM4 (see Table 2) and are close to the respective values obtained from the ERBE experiment (Barkstrom et al. 1990). A detailed discussion of the ECHAM4 TOA radiation budget is given in Chen and Roeckner (1996).

The ECHAM4-calculated absorbed shortwave radiation at the surface is compared with the observation-based estimates at the 720 GEBA locations in Fig 5c. The bias in the absorbed solar radiation at the surface is substantially smaller than previously seen in ECHAM3 (compare Figs. 2c and 5c). In particular, the large overestimate at low latitudes, of the order of 40 Wm^{-2} in ECHAM3, is no longer present in ECHAM4. Rather, a slight tendency for underestimation is found. The meridional insolation gradient, which was too large in ECHAM3 at mid-latitudes, is

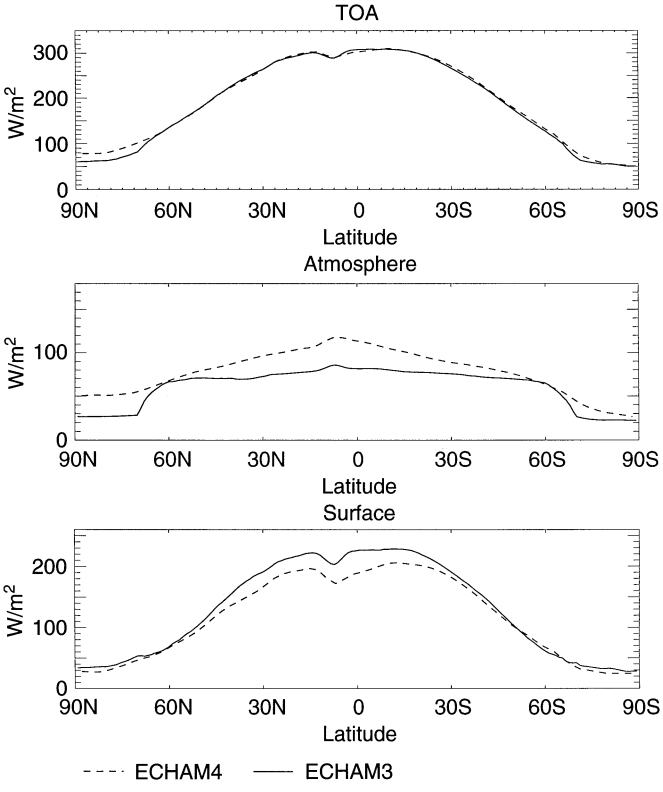

Fig. 4 Zonal mean shortwave absorption in the ECHAM3 and ECHAM4 GCMs at the top-of-atmosphere (TOA), within the atmosphere and at the surface. Units Wm^{-2}

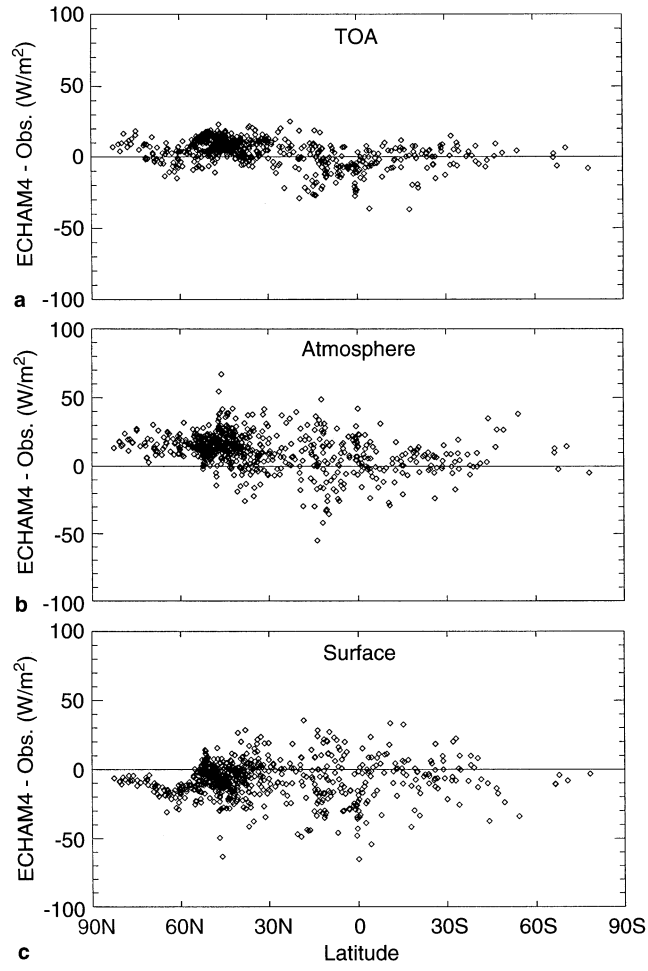

Fig. 5a–c As Fig. 2, but for ECHAM4

greatly reduced. Also on the regional scale, a significantly improved simulation of the surface insolation in ECHAM4 was noted in Wild et al. (1996) for Europe.

Figure 5c shows a tendency in ECHAM4 to underestimate the surface absorption at high latitudes. However, 77% of the Earth's surface is located between 50 °N and 50 °S, where the surface absorption is in good agreement with observations in ECHAM4 but substantially overestimated in ECHAM3. This may indicate that the 147 Wm^{-2} global mean surface absorption calculated in ECHAM4 is closer to reality than the 164 Wm^{-2} calculated in ECHAM3 or the values of other GCMs given in Fig. 1.

The mean bias between the model-calculated and observed surface absorption at the 720 sites, zonally weighted, is $-6\ Wm^{-2}$ for ECHAM4, while $+12\ Wm^{-2}$ in ECHAM3. This favors a best estimate of global mean shortwave surface absorption near 153 Wm^{-2}. This value is in line with other works suggesting a lower surface solar absorption than typically found in GCMs: 142 Wm^{-2} based on surface observations (Ohmura and Gilgen 1992) and 157 Wm^{-2} based on a satellite derived climatology (Li and Leighton 1993).

In Fig. 5b, differences between the atmospheric absorption as calculated in ECHAM4 and derived from observations are displayed. Compared to the ECHAM3 atmospheric shortwave absorption (Fig. 2b), the ECHAM4 atmospheric absorption is in better agreement with the observations. In particular, the substantial underestimation of atmospheric absorption at low latitudes is completely eliminated. Rather, a tendency towards overestimation of atmospheric absorption is found in ECHAM4, particularly at higher latitudes, which is responsible for the somewhat underestimated absorption at the surface. The overall overestimation of shortwave atmospheric absorption in ECHAM4 is, however, significantly smaller than its underestimation in ECHAM3. This suggests that the 90 Wm^{-2} global mean atmospheric absorption of ECHAM4 may be more realistic than the 71 Wm^{-2} of ECHAM3 given in Table 2. Taking into account the zonally weighted biases between the two models and the direct observations, the best estimate of global mean atmospheric shortwave absorption may be close to 85 Wm^{-2}, consideraby higher than in most current GCMs (see Fig. 3).

Figures 2 and 5 have shown that the improvements in the calculated surface fluxes in ECHAM4 compared to ECHAM3 are predominantly the result of a revised partitioning of shortwave absorption between the atmosphere and surface rather than due to changes in the absorption in the climate system as a whole. As can be inferred from Table 2, the increased atmospheric absorption in ECHAM4 is due to both increased clear-sky and cloud absorption of almost equal amounts: 9 Wm^{-2} of the 19 Wm^{-2} enhanced atmospheric absorption in ECHAM4 are due to an increased absorption of solar radiation in the cloud-free atmosphere (ECHAM3 63 Wm^{-2}, ECHAM4 72 Wm^{-2}), while the remainder of the 19 Wm^{-2} difference results from the enhanced absorption of the ECHAM4 clouds. The changes in clear- and cloudy-sky absorption are discussed in the following paragraphs.

5.2 Cloud-free atmosphere

Global mean values of solar radiation absorbed in the cloud-free atmosphere of a number of GCMs are given in Fig. 6. It is noteworthy that differences of up to 20 Wm^{-2} already exist in the GCM-calculated atmospheric clear-sky absorption. The GCM-calculated absorption in the cloud-free atmosphere depends, on one hand, on the formulation of the radiation scheme, and, on the other hand, on the distribution of absorbers and scattering particles which enter the radiative transfer calculations.

Water vapor is the principal absorber of solar radiation in the cloud-free atmosphere. Both ECHAM4 and ECHAM3 generally agree with the satellite-observed abundance of water vapor (Chen et al. 1996). No major differences exist in the vertically integrated water vapor content of the ECHAM3 and ECHAM4 atmospheres on the global and zonal scale, as shown in Fig. 7. Globally, the ECHAM4 atmosphere is slightly drier (3%) than the ECHAM3 atmosphere, and nevertheless more absorbing. Thus, atmospheric water vapor concentration cannot explain the 9 Wm^{-2} increase in clear-sky absorption in ECHAM4.

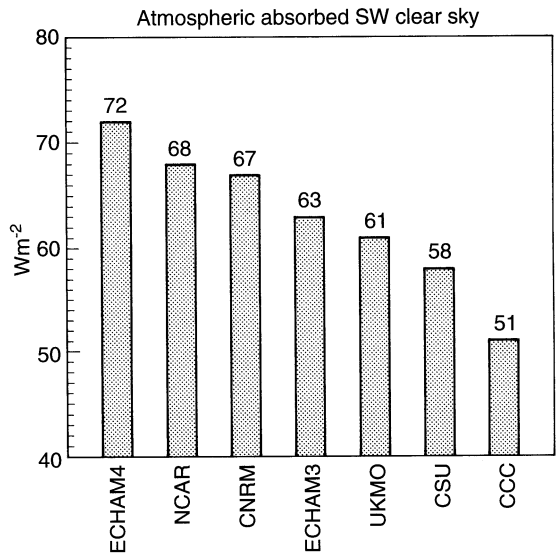

Fig. 6 Global annual mean absorbed shortwave radiation in the cloud-free atmosphere ("clear sky") in various GCMs. *CNRM* value from M. Déqué (personal communication, based on the ARPEGE model), *UKMO* value from R. Stratton (personal communication, based on model version HadAM2b), *NCAR*, *CSU*, *CCC* values from Li et al. (1997)

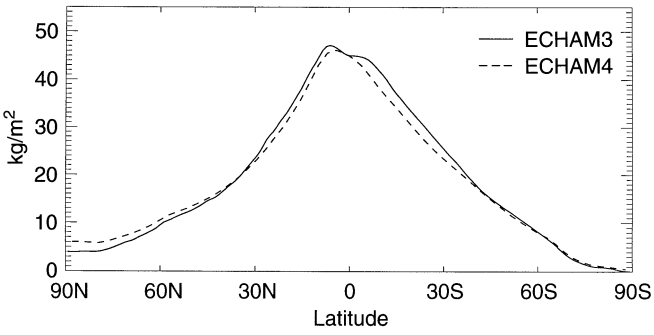

Fig. 7 Vertically integrated atmospheric water vapor (zonal annual mean), calculated with ECHAM3 and ECHAM4. Units kgm^{-2}

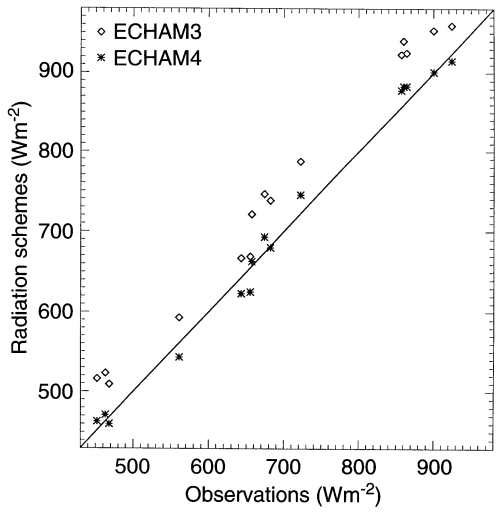

Fig. 8 Incoming shortwave radiation at the surface under clear-sky conditions at noon: Stand-alone calculations with the ECHAM3 and ECHAM4 radiation schemes with prescribed atmospheric temperature and humidity profiles from radiosonde launches versus synchronous surface radiation measurements. Radiosonde data and radiation measurements from Payerne, Switzerland. Units Wm^{-2}

The prescribed distribution and radiative properties of aerosols have not been changed from ECHAM3 to ECHAM4 and so can also not explain the differences in the fluxes, as discussed lates. Therefore, rather than differences in the GCM provided input to the radiation schemes, differences in the radiation schemes themselves seem to cause the discrepancies in the calculated fluxes under cloud-free conditions.

Thus, the clear-sky performance of the ECHAM3 and ECHAM4 radiation schemes is compared separately from the GCMs in stand-alone mode. This is done using prescribed atmospheric profiles of temperature and humidity from radiosonde data as input to the radiation scheme. This allows a representative comparison of the model-calculated surface fluxes with in-situ measurements. This procedure was applied in Wild et al. (1995a) to the ECHAM3 radiation scheme and revealed a substantial overestimation of the clear-sky insolation at the surface. Here the same procedure is applied to the ECHAM4 radiation scheme. The observational data (radiosonde profiles, surface radiation measurements) stem from the Swiss aerological station at Payerne which is run by the Swiss Meteorological Institute. The results of the stand-alone calculations with the ECHAM3 and ECHAM4 radiation schemes and the respective surface observations for a number of clear-sky situations are compared in Fig. 8. The calculations and measurements have been performed at noon local time, thus representing daily maximum values. The calculated irradiances of the two radiation schemes differ substantially despite identical input. The ECHAM4-calculated fluxes agree significantly better with observations than the ECHAM3 fluxes and no longer overestimate the clear-sky irradiance. The mean for the cases in Fig. 8 is 700 Wm^{-2} for ECHAM3, 650 Wm^{-2} for ECHAM4 and 647 Wm^{-2} for the observed fluxes. Thus, the ECHAM4 radiation scheme is very close to the observations (within measurement uncertainty which is estimated at 2% for single measurements), while the ECHAM3 scheme overestimates the surface fluxes substantially, by 50 Wm^{-2}. Note that these values are differences under daily maximum insolation at noon and should not be misinterpreted as mean climatological differences which are smaller: integrated over the whole diurnal cycle these differences reduce to approx. 10 Wm^{-2}. The differences in the (one-dimensional) stand-alone calculations are therefore consistent with the 9 Wm^{-2} difference in the calculated shortwave clear-sky budgets of the (three dimensional) ECHAM4 and ECHAM3 experiments (see Table 2). This confirms that the differences between the shortwave clear-sky budgets of the two models are predominantly caused by the radiation schemes rather than by differences in the composition of the model atmospheres.

More insight into the differences between the clear-sky computations of the ECHAM3 and ECHAM4 radiation schemes can be gained by a comparison of the individual spectral bands of the two models. The dimensions of the shortwave spectral intervals are given in Table 1. Although the number of bands are different in the two models, the separation between the visible band and the near-infrared bands is at the same wavelength (0.68 μm, see Table 1). This allows a direct comparison of the visible bands of the two schemes, while the single near-infrared band of ECHAM4 has to be compared with the sum of three near-infrared bands of ECHAM3. This is shown in Figs. 9 and 10 for the calculated clear-sky fluxes at the surface for the cases used previously in Fig. 8. In the visible bands, the clear-sky fluxes of the two models are almost identical, the difference is virtually zero (Fig. 9). This also confirms that the effects of aerosols are identical in the two models. Since the models calculate identical fluxes in the visible bands, the differences between the two

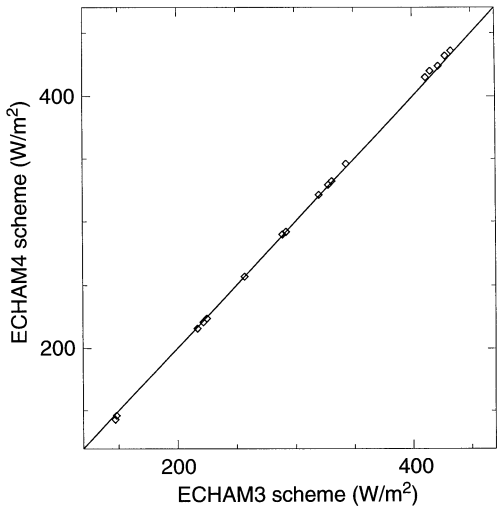

Fig. 9 Incoming shortwave flux at the surface in the visible part of the spectrum (0.2–0.7 μm) calculated by the ECHAM3 and ECHAM4 radiation schemes in stand-alone mode for the clear-sky cases used in Fig. 8

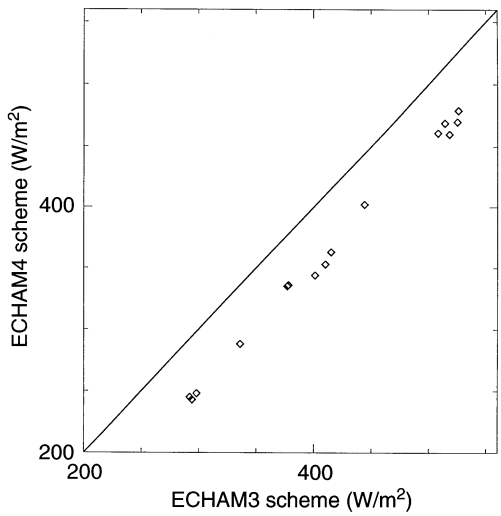

Fig. 10 As Fig. 9, but for the near-infrared part of the spectrum (0.7–4.0 μm)

schemes must be due to differences in the near-infrared bands. In fact, large differences can be seen in Fig. 10, where the sum of the fluxes in the three near-infrared bands of ECHAM3 are compared with the corresponding flux in the ECHAM4 band. The ECHAM3 scheme calculates substantially higher near-infrared fluxes at the surface than ECHAM4, i.e. the near-infrared absorption of solar radiation in the ECHAM4 scheme is considerably larger than in ECHAM3. In the near-infrared, water vapor is the dominant absorber. The larger water vapor absorption of ECHAM4 is derived from a more recent spectroscopic dataset. The ECHAM3 radiation scheme was based on spectroscopic data of an early LOWTRAN version (LOWTRAN3, Selby and McClatchey 1975), while the water vapor absorption bands of the ECHAM4 scheme are derived from the AFGL spectroscopic dataset (Rothman et al. 1992). Models based on early LOWTRAN data have been shown to underestimate water vapor absorption compared to models based on AFGL data (Fouquart et al. 1991).

It may be argued that the increased absorption in the cloud-free atmosphere in ECHAM4 is related to the coarse spectral resolution of the Morcrette scheme with only two bands in the shortwave (see Table 1). Therefore, a sensitivity study is conducted with the number of spectral bands increased up to 15. Atmospheric clear-sky absorption calculated for the cloud-free subarctic winter and tropical standard atmospheres is shown in Table 3 for various numbers of spectral bands. The results are normalized with the absorption calculated at the highest spectral resolution (15 bands). A small increase in clear-sky absorption with decreasing band number can be noted, with a maximum difference of 3% between the 2 bands and 15 bands resolution in both cases (Table 3). However, this corresponds to a difference of only 2 Wm^{-2} in the global mean clear-sky absorption, which can be attributed to the coarse spectral resolution. Most of the 9 Wm^{-2} difference in clear-sky absorption is therefore considered to be due to differences in water vapor absorption rather than numerical effects of spectral band resolution (these effects will not be negligible, however, in the case of cloud absorption, as will be shown in the next section).

To summarize, the stand-alone validation against observations indicates that the clear-sky shortwave radiative transfer is realistically captured in ECHAM4. This suggests that the 72 Wm^{-2} in Table 2 is a reasonable value for solar absorption in the cloud-free atmosphere and indicates that an underestimated absorption of solar radiation in the cloud-free atmosphere may be a problem common in many GCMs (see Fig. 6). Thus, an increased clear-sky absorption, as in ECHAM4, may contribute significantly to the reduction of discrepanices between calculated and observation-based estimates of solar absorption in the atmosphere.

Table 3 Atmospheric clear-sky absorption of solar radiation, calculated with the Morcrette (1991) radiation code with different numbers of spectral bands in the near-infrared. Results are based on the tropical and subarctic winter standard atmosphere, and are normalized to the absorption calculated with 15 spectral bands

Number of spectral bands	15	4	3	2
Tropical case	1	1.005	1.010	1.034
Subarctic winter case	1	1.010	1.012	1.033

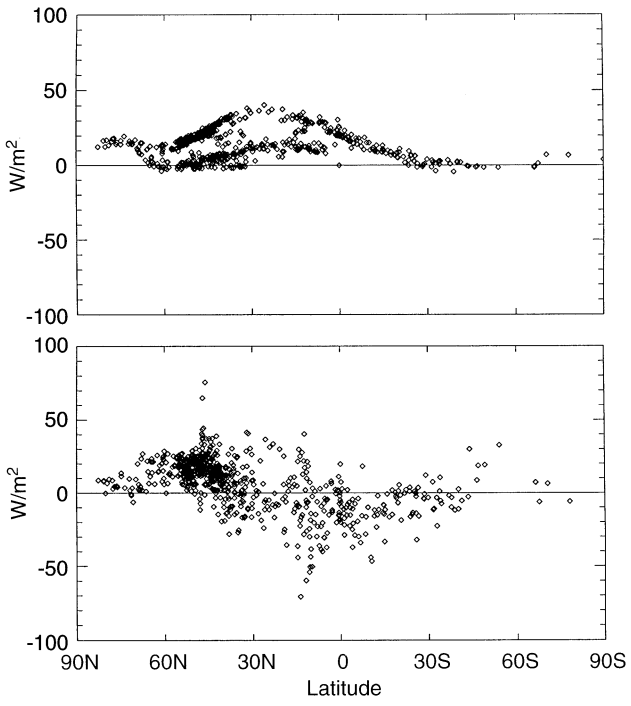

Fig. 11 a Differences between ECHAM4 and ECHAM3-calculated shortwave absorption in the cloud-free atmosphere at the 720 GEBA sites as function of latitude. **b** Differences between ECHAM3-calculated atmospheric shortwave absorption, increased by the additional ECHAM4 clear-sky absorption of **a**, and observation-derived absorption at the 720 GEBA sites as function of latitude

Differences between the atmospheric clear-sky absorption calculated by ECHAM4 and ECHAM3 at the 720 GEBA sites are explicitly shown in Fig. 11a. To illustrate the impact of the increased atmospheric clear-sky absorption, the extra ECHAM4 clear-sky absorption shown in Fig. 11a has been added to the ECHAM3 atmospheric all-sky absorption at each GEBA site and compared to the observation-derived values (Fig. 11b). Compared to the ECHAM3 atmospheric absorption in Fig. 2b, the additional ECHAM4 clear-sky absorption results in an improved simulation of atmospheric absorption and considerably reduces the bias in atmospheric absorption at low latitudes. Assuming an accurate clear-sky simulation in Fig. 11b, the remaining biases may be attributed to other effects such as deficiencies in the calculated cloud absorption.

5.3 Cloudy atmosphere

Two factors determine the interaction of clouds and radiation, namely the cloud radiative properties, and the spatial dimensions of the clouds, i.e., the cloud fraction. In the ECHAM4 simulation, the global mean cloud fraction is 0.60, which is substantially larger than in ECHAM3 (0.52). The larger cloud fraction in ECHAM4 is in better agreement with observational estimates, which amount to 0.61 based on surface observations (Warren et al. 1986) and to 0.63 based on satellite observations (Rossow and Gardner 1993). The zonal simulation of cloud fraction over land, where most of the radiative flux measurements are available, is compared in Fig. 12 with the surface-based climatology of Warren et al. (1986). ECHAM4 captures the zonal distribution of the cloud fraction more accurately than ECHAM3. The improvement in ECHAM4 is evident at most latitudes. In particular at low latitudes, the agreement with the observations is excellent and the underestimated cloud amount found in ECHAM3 is no longer present in ECHAM4.

Since the shortwave balance at the TOA is very similar in ECHAM3 and ECHAM4 in the zonal mean (see Fig. 4), the effect of increased cloud fraction in ECHAM4 on the shortwave radiative fields is predominantly due to an increase in the cloud absorption rather than an increase in the reflection back to space. This can be quantified in the shortwave atmospheric cloud radiative forcing (CRF), i.e., the difference between the solar radiation absorbed in the atmosphere with and without clouds: the shortwave atmospheric CRF is enhanced from $8\,\mathrm{Wm}^{-2}$ in ECHAM3 to $18\,\mathrm{Wm}^{-2}$ in ECHAM4 on the global average, i.e., an increase of $10\,\mathrm{Wm}^{-2}$ (Table 2). A substantially higher cloud-absorption than previously assumed has been advocated in several recent observational studies (e.g., Cess et al. 1995; Ramanathan et al. 1995), and is, to date, a highly controversial issue. The increased cloud absorption in ECHAM4 has the following origins:

1. As previously discussed, ECHAM4 has an increased cloud fraction of 0.60 compared to 0.52 in ECHAM3. This effect alone results in an additional absorption of $3\,\mathrm{Wm}^{-2}$ in the global mean.

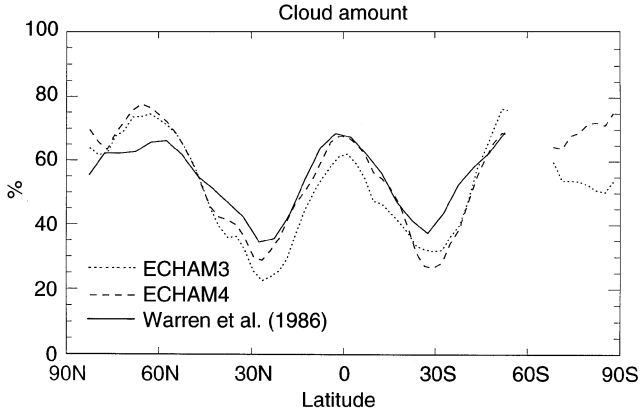

Fig. 12 Zonal annual mean cloud amount over land: simulations with ECHAM3 and ECHAM4 compared to the climatology of Warren et al. (1986). Units percentage of cloud amount

2. ECHAM4 simulates substantially more low-level clouds than ECHAM3. Low-level clouds are characterized by high liquid water content and therefore high optical thickness and absorption.
3. The ECHAM4 radiation scheme resolves only two bands in the shortwave spectrum, whereas ECHAM3 has 4 bands (see Table 1). While we have shown previously that this has no major impact on the calculated clear-sky absorption, it can no longer be neglected when cloud absorption is involved. This is illustrated in stand alone-calculations with different numbers of spectral bands as before in Sect. 5.2, but now additionally with a convective cloud inserted in the atmospheric column. The increase in atmospheric absorption with decreasing band number is substantial, in contrast to the clear-sky calculations before. The difference in absorption between the two bands and 15 bands versions amounts to 15% for the tropical and 14% for the subarctic winter case (Table 4). Thus, a substantial amount of spurious cloud absorption is introduced through the coarse spectral resolution in the near-infrared. Similar results were obtained by Slingo (1989) who showed that a reduction in the number of shortwave bands below 4 can cause an artificial increase in the fraction of the spectrum available for absorption, resulting in a reduction of the single scattering albedo averaged over large bandwidths.

Thus, the increased cloud absorption in ECHAM4 is, contrary to the clear-sky absorption, predominantly a numerical artefact. It is beyond the scope of this paper to give a physical explanation for a possible increase in cloud absorption. Rather, we focus here on the question, to what extent an increase in cloud absorption (however generated) is consistent with our dataset of direct observations. To quantify the effects of clouds and for comparison with the studies of Cess et al. (1995), we adapt their concept of the cloud radiative forcing ratio R, i.e., the ratio of the cloud radiative forcing at the surface to the cloud radiative forcing at the TOA. R is a measure of the impact of clouds on the absorption within an atmospheric column, e.g., when R is 1, it states that the inclusion of clouds has no net effect on the solar absorption within an atmospheric column. Cess et al. (1995) and Ramanathan et al. (1995) suggested that R is close to 1.5 as opposed to 1.1 found typically in GCMs, implying a higher absorption of solar radiation by clouds than assumed in current models. In ECHAM3, R is 1.16 as can be inferred from the TOA and surface cloud radiative forcings in Table 2. In ECHAM4, R is increased to 1.35, i.e., half way between typical GCM values and the value suggested by Cess et al. (1995). These comparisons with observational data indicate that both all-sky and clear-sky shortwave fluxes, as well as cloud amount, are more consistent with observations in ECHAM4 than in ECHAM3 over large parts of the globe. As a first approximation, this suggests that also an R value of 1.35 as in ECHAM4 may be more appropriate than the 1.16 in ECHAM3. However, a further increase of R up to 1.5 would definitely lead to a surface insolation of ECHAM4 which is too small at the GEBA sites, if not the clear-sky absorption or cloud amount would be simultaneously reduced (for which there is no evidence from these validations). Rather, 1.35 seems an upper limit when considering that the total atmospheric absorption of solar radiation in ECHAM4 already seems somewhat high (see Fig. 5b), and the absorption by aerosols might not be considered to the full extent in this model, as discussed later.

For a more differentiated interpretation of the biases between model-calculated and observed absorption found in Figs. 2b, 5b, 11b, R is shown as function of latitude in Fig. 13. R is enhanced in ECHAM4 compared to ECHAM3 at most latitudes, with a maximum in the tropics. Exceptions are the zones around 60 °N/S, where R in ECHAM3 reaches or even exceeds the ECHAM4 values. The zonal differences in R between ECHAM3 and ECHAM4 are in line with the zonal distribution of cloud water in the two models (Fig. 14). The large R in ECHAM3 around 60 °N/S is related to a maximum of cloud water in these areas.

Figure 11b gave evidence that the increased ECHAM4 clear-sky absorption alone may not completely remove the underestimation of atmospheric absorption at low latitudes. With the additional increase

Table 4 As Table 3, but with a convective cloud inserted into the atmospheric column

Number of spectral bands	15	4	3	2
Tropical case	1	1.020	1.054	1.157
Subarctic winter case	1	1.022	1.067	1.141

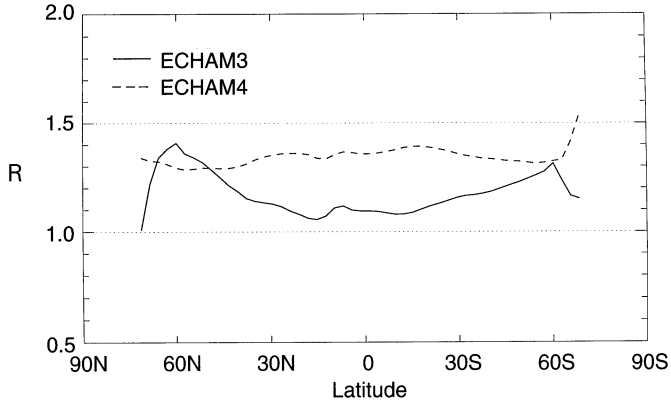

Fig. 13 Ratio (R) of shortwave cloud radiative forcing at the surface to that at the top-of-atmosphere calculated with ECHAM3 and ECHAM4 (zonal annual mean)

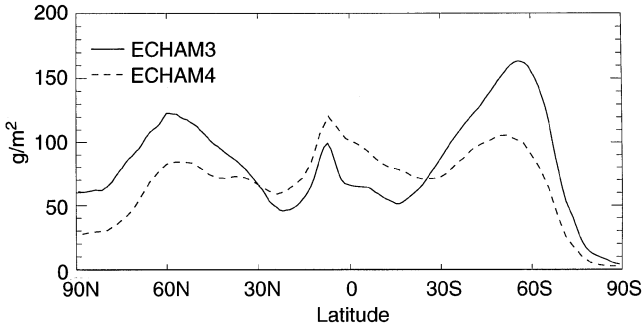

Fig. 14 Vertically integrated cloud water calculated with ECHAM3 and ECHAM4 (zonal annual mean). Units gm^{-2}

in the cloud absorption in ECHAM4 at these latitudes, the biases compared to the observations are reduced. For these latitudes, Figs. 2b, 5b and 11b suggest that a certain increase in cloud absorption, as present in ECHAM4, is not in conflict with observations. This implies that the possibility of higher R values around 1.3–1.4 as in ECHAM4 at these latitudes (Fig. 13) may not be ruled out. A further increase in R beyond 1.4, however, is likely to result in an atmosphere that is too opaque, considering that the atmospheric absorption calculated with ECHAM4 already shows a slight tendency towards overestimation rather than underestimation (Fig. 5b). Furthermore, some of the differences between GCM-calculated and observed atmospheric absorption in equatorial areas may be due to the presence of large loadings of aerosols related to biomass burning near the observation sites, which are not considered in the GCM calculations. Konzelmann et al. (1996) suggest that black carbon aerosols can have a significant impact on the incoming shortwave radiation at GEBA sites in Equatorial Africa. Quantitative estimates of the effects of strongly absorbing aerosols are still afflicted with large uncertainties. Nevertheless, at such locations, we cannot exclude the possibility that strongly absorbing aerosols rather than cloud absorption are causing the higher observed than calculated atmospheric absorption, as also pointed out by Li et al. (1995b) and Li et al. (1997).

At higher latitudes, around 60 °N/S, these comparisons with observations (Figs. 2b, 5b) indicate that cloud absorption is rather too high in both ECHAM3 and ECHAM4, and give no evidence that R should be as high as in the two models. Instead, only a significantly lower R value close to 1 rather than the value near 1.3 presently found in both ECHAM3 and ECHAM4 around 60 °N/S would reduce the discrepancies in Figs. 2b, 5b, 11b. Our results are in line with the study of Li et al. (1995b), who also found evidence for a zonal differentiation of R with higher values in low latitudes, but low values near 1 at high latitudes.

6 Longwave radiation

The longwave balance at the Earth's surface consists of the upward thermal emission from the surface and the downwelling atmospheric emission absorbed by the surface (downward longwave radiation). While the modelling of the thermal emission of the surface is straightforward according to the Stefan-Boltzmann law, the downward longwave flux has to be determined by comprehensive radiative transfer calculations, which take into account the complex radiative characteristics of the atmosphere.

The global mean downward longwave radiation calculated in different GCMs largely varies, as can be inferred from Fig. 15. The values shown cover a range of as much as 40 Wm^{-2}. ECHAM4 simulates a significantly higher global mean downward longwave flux compared to ECHAM3 and other GCMs. Wild et al. (1995a) presented evidence that the downward longwave radiation at the surface in ECHAM3 and other GCMs is underestimated by at least 10 Wm^{-2}. This has also been reported more recently by Garratt and Prata (1996).

Wild et al. (1995a) identified the clear-sky performance of the radiation scheme as a major source of the underestimation. Using a stand-alone version of the radiation scheme they showed that the ECHAM3 radiation scheme calculates a longwave downward flux which is too small, of the order of 10 Wm^{-2} under clear-sky conditions.

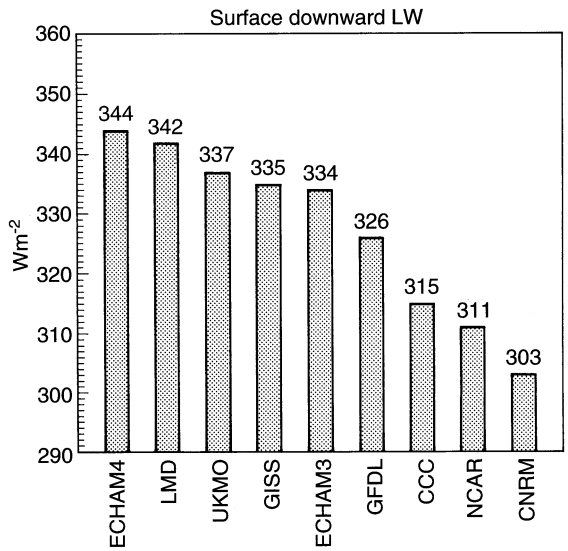

Fig. 15 Global mean downward longwave radiation at the surface calculated with ECHAM3, ECHAM4 and a number of other GCMs. *NCAR*, *GFDL*, *GISS* values from Gutowski et al. (1991), *CCC* value from Boer (1993), *LMD* value from J. Polcher (personal communication, based on model version LMD6), *CNRM* value from M. Déqué (personal communication, based on the ARPEGE model), *UKMO* value from R. Stratton (personal communication, based on model version HadAM2b). Units Wm^{-2}

The longwave part of the ECHAM4 radiation scheme is based on the radiation code of the ECMWF Cycle 43 model (Morcrette 1991). The original ECMWF scheme includes the water vapor continuum formulation of Roberts et al. (1976). This parametrization was modified to include temperature-weighted band averages of *e*-type continuum and a band dependent ratio of (*p*–*e*)-type to *e*-type continuum absorption following Ma and Tipping (1992) (Giorgetta and Wild 1995). These modifications result in an increase in the downward longwave radiation of 10 Wm^{-2} compared to the original Morcrette scheme.

The clear-sky performance of the ECHAM3 and ECHAM4 longwave radiation schemes is assessed in the following. Figure 16 compares downward longwave fluxes calculated with the ECHAM3 and ECHAM4 radiation schemes with in-situ observations. These calculations were again performed in stand-alone mode, with prescribed atmospheric profiles of humidity and temperature from radiosondes. The calculations were undertaken for a number of clear-sky situations at midnight using observational data from the Swiss aerological station at Payerne. Figure 16 shows that the ECHAM4 radiation scheme calculates systematically higher downward longwave fluxes than the ECHAM3 scheme, in good agreement with observations. The average over the cases shown in Fig. 16 is 269.5 Wm^{-2} for the ECHAM3 scheme, 280.0 Wm^{-2} for the ECHAM4 scheme, and 278.4 Wm^{-2} observed. The bias of the ECHAM4 scheme (1.5 Wm^{-2}) is well within the measurement error.

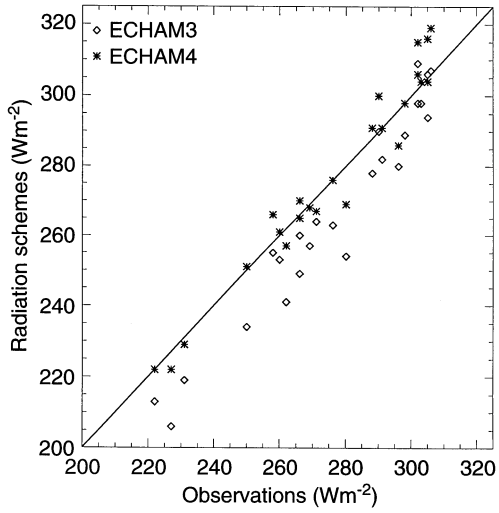

Fig. 16 Incoming longwave radiation at the surface under clear-sky conditions at midnight: stand-alone calculations with the ECHAM3 and ECHAM4 radiation schemes with prescribed atmospheric temperature and humidity profiles from radiosonde launches versus synchronous surface radiation measurements. Radiosonde data and radiation measurements from Payerne, Switzerland. Units Wm^{-2}

The 10.5 Wm^{-2} increase in the clear-sky flux of the ECHAM4 radiation scheme compared to the ECHAM3 scheme found in the stand-alone mode is reflected in the global mean values of the full three-dimensional GCM simulations: according to Table 2, the global mean clear-sky downward longwave radiation is 12 Wm^{-2} higher in ECHAM4 than in ECHAM3. This table also shows that the all-sky and clear-sky global mean values are increased by a very similar amount in ECHAM4. Thus, on the global scale, the increase in the downward longwave radiation is mainly due to the increased downward emission of the cloud-free atmosphere, while the surface longwave cloud radiative forcing (impact of clouds on downward longwave radiation) is similar in both model versions (see Table 2).

A number of stations monitoring the downward longwave fluxes are available from the Global Energy Balance Archive. These sites have been used in Wild et al. (1995a) to document the systematic underestimation of the ECHAM3-calculated downward longwave fluxes. The climatological annual cycles of downward longwave radiation calculated with ECHAM4 at these sites are compared with ECHAM3 and the observations in Fig. 17. ECHAM4 shows at most sites an increased flux which reproduces the observed annual cycle more accurately than ECHAM3.

More long-term observations are urgently needed to improve the data basis for the assessment of the GCM simulated downward longwave radiation. A major effort in this direction is currently underway with the establishment of the Baseline Surface Radiation Network (BSRN), which aims to achieve long-term monitoring of surface radiative fluxes at selected sites in different climatic regimes, equipped with instruments of highest possible accuracy (Ohmura et al. 1998). Preliminary results of a comparison with a first series of data from a number of these stations indicate that zonally, the ECHAM4-calculated downward longwave radiation shows a tendency towards overestimation in lower latitudes and underestimation in higher latitudes, which needs further analysis. Nevertheless, the sum of the available observational data and the stand-alone calculations with the radiation scheme indicate that, globally, the ECHAM4-calculated downward longwave radiation of 344 Wm^{-2} is a realistic value. Note that the ECHAM4 model exhibits a significantly high global mean downward longwave flux as compared to other GCMs (Fig. 15). This further emphasizes a likely underestimation of the downward longwave radiation typically found in current GCMs as evidenced by Wild et al. (1995a) and Garratt and Prata (1996). The ECHAM4-simulated 344 Wm^{-2} of downward longwave radiation also comes close to the 350 Wm^{-2} estimated by Ohmura and Gilgen (1992), and the 348 Wm^{-2} derived from satellite products by Rossow and Zhang (1995). The increased downward longwave flux reduces the net

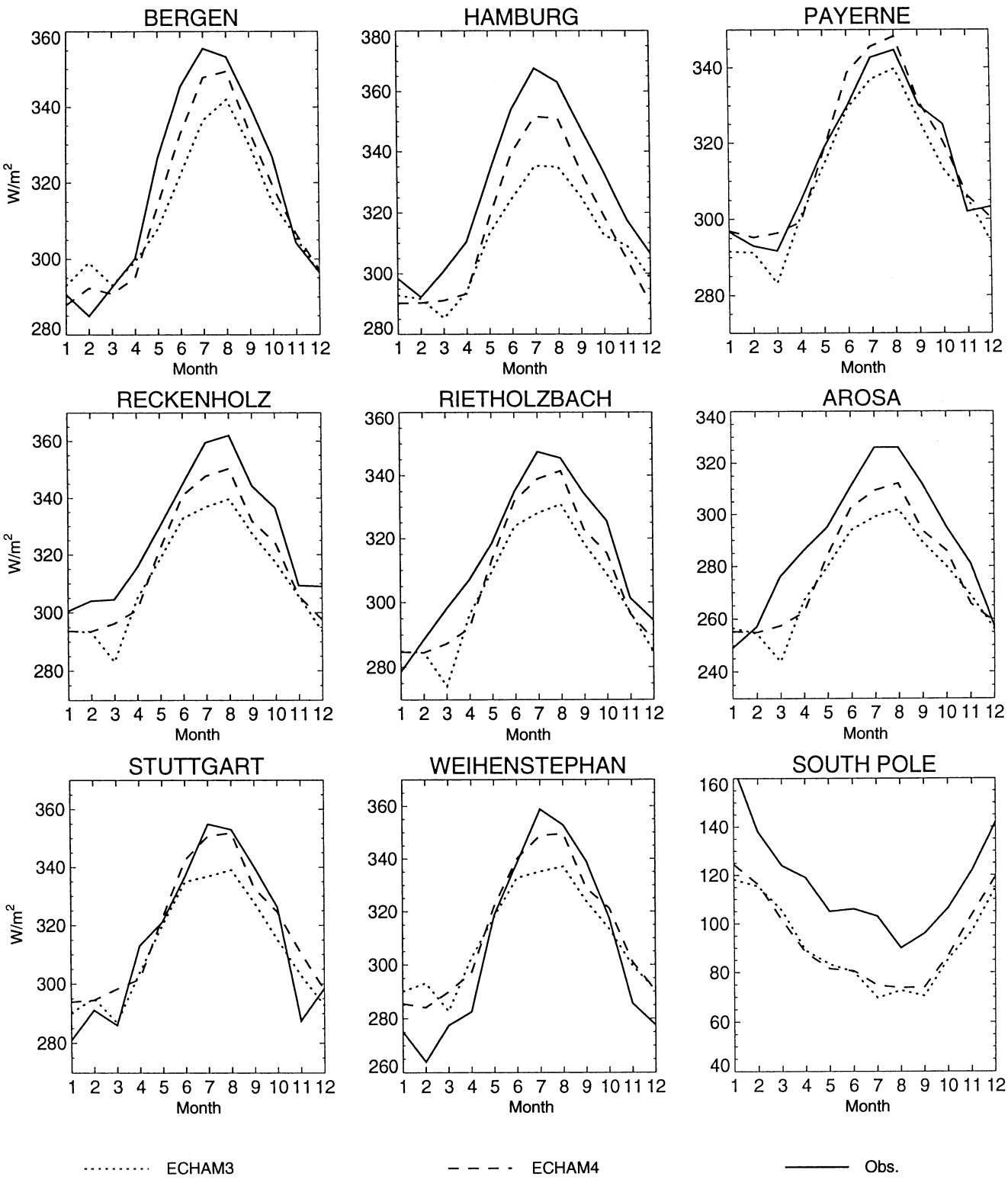

Fig. 17 Annual cycles of model-calculated (ECHAM3, ECHAM4) and observed surface downward longwave radiation at a number of stations from the Global Energy Balance Archive. Units Wm^{-2}

longwave cooling at the surface from $-63\ Wm^{-2}$ in ECHAM3 to $-53\ Wm^{-2}$ in ECHAM4, as shown in Table 2 (the global mean surface temperature, and accordingly, the upward longwave flux at the surface, changed insignificantly from ECHAM3 to ECHAM4).

7 Surface net radiation and global hydrological cycle

With the net longwave cooling reduced by 10 Wm^{-2}, the reduction of shortwave surface absorption by 17 Wm^{-2} is partially balanced, such that the available energy at the surface (surface net radiation) is reduced only by 7 Wm^{-2} in ECHAM4 globally. Consequently, the latent heat flux (the energy equivalent of the evaporation), which is driven by the surface net radiation, is also not substantially reduced in ECHAM4. This ensures that the associated intensity of the global hydrological cycle does not become unrealistically weak (the evaporation is equal to the precipitation on a global average). The global mean precipitation in ECHAM4 amounts to 83 mm/month, while observed values range from 80 to 100 mm/months (Jaeger 1976; Legates and Willmott 1990; Spencer 1993). Reducing only the surface shortwave absorption in GCMs (by enhancing the atmospheric clear-sky or cloud absorption) without touching the longwave fluxes, on the other hand, may lead to a surface net radiation which is too small and accordingly, to a global hydrological cycle which is too weak.

An indirect indication of higher downward longwave radiation than previously assumed therefore comes from the demand to reduce the surface shortwave absorption in the models without reducing the intensity of the global hydrological cycle.

To summarize, the global mean surface net radiation in ECHAM4 of 95 Wm^{-2} is not substantially different from other GCMs despite the reduced surface shortwave absorption (compare compilation of surface net radiation values of several GCMs in Wild et al. 1995a). However, while the surface net radiation in ECHAM3 and other models is only realistic due to an error cancellation between an overestimated surface insolation and underestimated downward longwave radiation as evidenced in Wild et al. (1995a), in ECHAM4 it is not only the net balance that is consistent with observations, but also its shortwave and longwave components.

8 Conclusions

The surface and atmospheric radiation budgets as calculated in GCMs have been assessed using a comprehensive dataset of direct measurements at the surface and the top of the atmosphere. Based on a comparison of the ECHAM3 GCM with more than 700 observation sites evidence has been presented that current GCMs typically underestimate the absorption of solar radiation in the atmosphere.

The surface and atmospheric radiation budgets simulated with ECHAM4 show significantly different values compared to ECHAM3 and other GCMs. The shortwave surface absorption in ECHAM4 is substantially reduced to 147 Wm^{-2}, due to a higher atmospheric absorption of 90 Wm^{-2}, thereby reducing the biases compared to the observations. The increased atmospheric absorption in ECHAM4 is related to a higher absorption in both clouds and cloud-free atmosphere.

Based on stand-alone calculations with the radiation scheme, evidence has been presented that the increased absorption in the cloud-free atmosphere (global mean value of 72 Wm^{-2}) is in line with synchronous surface measurements, and is related to enhanced water vapor absorption compared to the ECHAM3 scheme. This underlines the importance of an accurate simulation of the absorption of solar radiation in the cloud-free atmosphere to reduce the problem of excessively transparent GCM atmospheres (see also Wild and Liepert 1998).

The increase in cloud absorption in ECHAM4 has been shown to be predominantly a numerical artefact caused by the coarse spectral resolution of the shortwave radiation code, and therefore provides no physical explanation for the "anomalous" cloud absorption problem. Yet, it has been shown that quantitatively, an increase in cloud absorption of magnitude as in ECHAM4 (up to a cloud radiative forcing ratio R of 1.3–1.4) leads, at low latitudes, to a reduction of the bias between calculated and observed total atmospheric absorption. This, however, does not rule out the possibility that other effects such as the inclusion of strongly absorbing aerosols could equally reduce this bias. At higher latitudes the data suggest a value of R close to 1.

Despite the reduced absorption of solar energy at the surface in ECHAM4 (10–30 Wm^{-2} smaller than in other GCMs), the net energy available at the surface is not substantially reduced and is still sufficient to maintain a realistic strength of the associated hydrological cycle. This is due to more available longwave energy, provided by an increased flux of downward longwave radiation. This increase is due to an enhanced atmospheric clear-sky emission of the ECHAM4 radiation scheme. The enhanced clear-sky downward longwave flux is in agreement with synchronous surface observations in stand-alone mode. The available surface observations from GEBA further support the larger downward longwave flux in ECHAM4, which, at 344 Wm^{-2}, is substantially higher than in many other GCMs.

Even though the ECHAM4 model may not provide a physical justification for all changes in its radiation budget, quantitatively, it comes closer to the comprehensive dataset of direct observations and minimizes two biases identified in the current generation of GCMs, i.e., a lack of absorption of solar radiation in the atmosphere, and an error balance between excessive shortwave heating and longwave cooling at the surface. The global annual mean all-sky and clear-sky radiation budgets considered as most realistic, based on the observations and model biases discussed in this study, are summarized in Fig. 18.

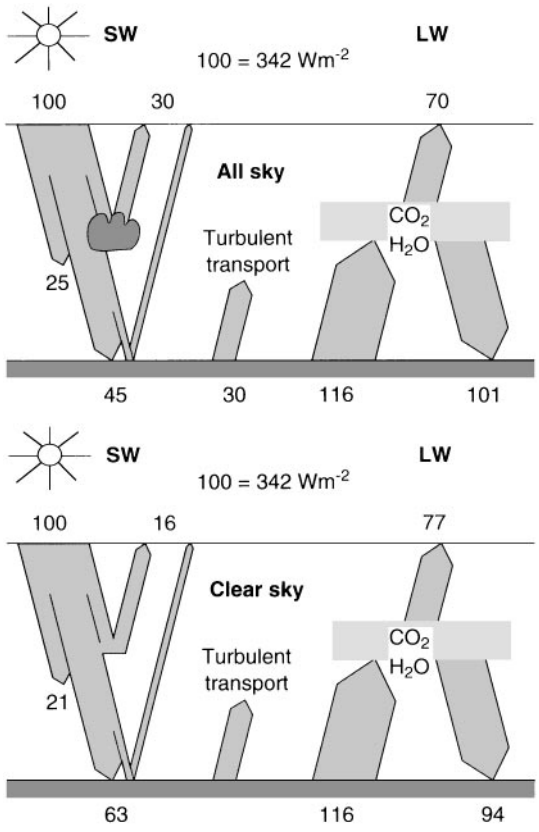

Fig. 18 Best estimates for global mean values of the earth's radiation budget for *all-sky* and *clear-sky* conditions, derived from model biases compared to a comprehensive set of direct observations. Units percentage of solar irradiance at the top-of-atmosphere

Acknowledgements The first author is indebted to Prof. L. Bengtsson for the possibility to frequently visit the MPI. Thanks to Drs. M. Déqué and R. Stratton for making available the output of the Météo-France and UKMO GCMs for comparative purposes within the framework of the EU project HIRETYCS. The Swiss Scientific Computing Center CSCS generously provided the necessary computer resources for the ECHAM3 and ECHAM4 simulations. The Swiss Meteorological Institute measured upper-air and surface data at the aerological station Payerne. The present work was financed through the Swiss National Science Foundation Grants National Research Program 31, Climate Change and Natural Hazards (Grant 4031-033250) and Priority Program Environment (SPP, Grant 5001-35179), and the EU project HIRETYCS supported by the Swiss Bundesamt für Bildung und Wissenschaft (BBW) Grant 95.0640.

References

Arking A (1996) Absorption of solar energy in the atmosphere: Discrepancy between model and observations. Science 273:779–782

Barker HW, Li Z (1995) Improved simulation of clear-sky shortwave radiative transfer in the CCC GCM. J Clim 8:2213–2223

Barkstrom BR, Harrison EF, Lee III RB (1990) Earth Radiation Budget Experiment. EOS 71:297–305

Boer GJ (1993) Climate change and the regulation of the surface moisture and energy budgets. Clim Dyn 8:225–239

Cess RD, Zhang MH, Minnis P, Corsetti L, Dutton EG, Forgan BW, Garber DP, Gates WL, Hack JJ, Harrison EF, Jing X, Kiehl JT, Long CN, Mocrette JJ, Potter GL, Ramanathan V, Subasilar B, Whitlock CH, Young DF, Zhou Y (1995) Absorption of solar radiation by clouds: observations versus models. Science 267:496–499

Chen CT, Roeckner E (1996) Validation of the earth radiation budget as simulated by the Max Planck Institute for Meteorology general circulation model ECHAM4 using satellite observations of the Earth Radiation Budget Experiment (ERBE). J Geophys Res 101:4269–4287

Chen CT, Roeckner E, Soden BJ (1996) A comparison of satellite observations and model simulations of column integrated moisture and upper tropospheric humidity. J Clim 9:1561–1585

Claussen M, Lohmann U, Roeckner E, Schulzweida U (1994) A global dataset of land-surface parameters. Max-Planck-Institut for Meteorology Rep 135

Darnell WL, Staylor WF, Gupta SK, Ritchey NA, Wilber AC (1992) Seasonal variation of surface radiation budget derived from International Satellite Cloud Climatology Project C1 data. J Geophys Res 97:15741–15760

Fouquart Y, Bonnel B (1980) Computations of solar heating of the Earth's atmosphere: a new parametrization. Beitr Phys Atmos 53:35–62

Fouquart Y, Bonnel B, Ramaswamy V (1991) Intercomparing shortwave radiation codes for climate studies. J Geophys Res 96:8929–8953

Garratt JR (1994) Incoming shortwave fluxes at the surface – a comparison of GCM results with observations. J Clim 7:72–80

Garratt JR, Prata A (1996) Downwelling longwave fluxes at continental surfaces- a comparison with GCM simulations and implications for the global land-surface radiation budget. J Clim 9:646–655

Gates WL (1992) AMIP: The atmospheric model intercomparison project. Bull Am Meteorol Soc 73:1962–1970

Geleyn JF, Preuss HJ (1983) A new data set of satellite-derived surface albedo values for operational use at ECMWF. Arch Meteor of Geophys Bioclim Ser A 32:353–359

Gilgen H, Wild M, Ohmura A (1997) Global Energy Balance Archive GEBA, World Climate Program – Water Project A7, Report 3: The GEBA version 1997 database. Zürcher Geograf Schr 74, Zürich, 105p (available from Geography Institute ETH, Winterthurerstr. 190, CH-8057 Zürich)

Gilgen H, Wild M, Ohmura A (1998) Means and trends of shortwave irradiance at the surface estimated from Global Energy Balance Archive data. J Clim 11:2042–2061

Giorgetta M, Wild M (1995) The water vapor continuum and its representation in ECHAM4. Max Planck Institute for Meteorology Rep 162, Hamburg, Germany

Gutowski WJ, Gutzler DS, Wang WC (1991) Surface energy balances of three general circulation models: implications for simulating regional climate change. J Clim 4:121–134

Hense A, Kerschgens M, Raschke E (1982) An economical method for computing radiative transfer in circulation models. Q J R Meteorol Soc 108:231–252

Jaeger L (1976) Monatskarten des Niederschlags fuer die ganze Erde. Ber Dtsch Wetterdienstes: 139, Offenbach

Kerschgens MU, Pilz E, Raschke E (1978) A modified two stream approximation for computations of the solar radiation budget in a cloudy atmosphere. Tellus 30:429–435

Konzelmann T, Cahoon DR, Whitlock CH (1996) Impact of biomass burning in Equatorial Africa on the downward surface shortwave irradiance: observations and calculations. J Geophys Res 101(D1):22833–22844

Legates DR, Willmott CJ (1990) Mean seasonal and spatial variability in gage-corrected global precipitation. Int J Climatol 10:111–127

Li Z (1998) Influence of absorbing aerosols on the inference of solar surface radiation budget and cloud absorption. J Clim 11:5–17

Li Z, Leighton HG (1993) Global climatologies of solar radiation budgets at the surface and in the atmosphere from 5 years of ERBE data. J Geophys Res 98 : 4919–4930

Li Z, Whitlock CH, Charlock TP (1995a) Assessment of the global monthly mean surface insolation estimated from satellite measurements using Global Energy Balance Archive data. J Clim 8 : 315–328

Li Z, Barker H, Moreau L (1995b) The variable effect of clouds on atmospheric absorption of solar radiation. Nature 376 : 486–490

Li Z, Moreau L, Arking A (1997) On solar energy disposition, Bull Am Meteorol Soc 78 : 53–70

Ma Q, Tipping RH (1992) A far wing line shape theory and its application to the foreign-broadened water continuum absorption. J Chem Phys 97 : 818–828

Morcrette JJ (1991) Radiation and cloud radiative properties in the European centre for medium range weather forecasts forecasting system. J Geophys Res 96 : 9121–9132

Morcrette JJ, Smith L, Fouquart Y (1986) Pressure and temperature dependence of the absorption in longwave radiation parameterizations. Beitr Phys Atmos 59 : 455–469

Ohmura A, Gilgen H (1992) Global Energy Balance Archive (GEBA, WCP-water A7) and new aspects of the global radiation distribution on the Earth's surface. In: S. Keevallik and O. Kärner (eds.) IRS '92, Current problems in atmospheric radiation. DEEPAK Publishing, pp 271–274, Hampton, Virginia

Ohmura A, Dutton E, Forgan B, Fröhlich C, Gilgen H, Hegner H, Heimo A, König-Langlo G, McArthur B, Müller G, Philipona R, Pinker R, Whitlock C, Wild M (1998) Baseline Surface Radiation Network (BSRN/WCRP), a new precision radiometry for climate research, Bull Am Meteorol Soc (in press)

Ramanathan V, Subasilar B, Zhang G, Conant W, Cess R, Kiehl J, Grassl H, Shi L (1995) Warm pool heat budget and shortwave cloud forcing: a missing physics? Science 267 : 499–503

Randall DA, Cess RD, Blanchet JP, Boer GJ, Dazlich DA, Del Genio AD, Deque M, Dymnikov V, Galin V, Ghan SJ, Lacis AA, Le Treut H, Li ZX, Liang XZ, McAveney BJ, Meleshko VP, Mitchell JFB, Mocrette JJ, Potter GL, Riskus L, Roeckner E, Royer JF, Schlese U, Sheinin DA, Slingo J, Sokolov AP, Taylor KE, Washington WM, Wetherald RT, Yagai I, Zhang MH (1992) Intercomparison and interpretation of surface energy fluxes in atmospheric general circulation models. J Geophys Res 97 : 3711–3725

Roberts RE, Selby JEA, Biberman LM (1976) Infrared continuum absorption by atmospheric water vapor in the 8–12 μm window. Appl Opt 15 : 2085–2090

Rockel B, Raschke E, Weyres B (1991) A parameterization of broad band radiative transfer properties of water, ice and mixed clouds. Beitr Phys Atmos 64 : 1–12

Roeckner E, Arpe K, Bengtsson L, Brinkop S, Dümenil L, Esch M, Kirk E, Lunkeit F, Ponater M, Rockel B, Sausen R, Schlese U, Schubert S, Windelband M (1992) Simulation of the present day climate with the ECHAM model: impact of model physics and resolution. Max Planck Institute for Meteorology Rep 93, Hamburg, 171p

Roeckner E, Arpe K, Bengtsson L, Christoph M, Claussen M, Dümenil L, Esch M, Giorgetta M, Schlese U, Schulzweida U (1996) The atmospheric general circulation model ECHAM4: model description and simulation of present day climate. Max Planck Institute for Meteorology Rep 218, Hamburg, 130 p

Rossow WB, Garder LC (1993) Validation of ISCCP cloud detections. J Clim 6 : 2370–2393

Rossow WB, Zhang YC (1995) Calculation of surface and top of atmosphere radiative fluxes from physical quantities based on ISCCP data sets. Part II: validation and first results. J Geophys Res 100 (D1) : 1167–1197

Rothman LS et al. (1992) HITRAN molecular database: Editions of 1991 and 1992. J Quant Spectros Radiat Transfer 48 : 469–507

Selby IEA, McClatchey RE (1975) Atmospheric transmittance from 0.25–28.5 μm, computer code LOWTRAN 3, AFCLR-TR-75–0255

Shettle EP, Fenn R (1976) Models of the atmospheric aerosols and their optical properties. AGARD Conf Proc 183, AGARD-CP-183

Slingo A (1989) A GCM parameterization for the shortwave radiative properties of water clouds. J Atm Sci 46 : 1419–1427

Spencer RW (1993) Global oceanic precipitation from MSU during 1979–1991 and comparisons to other climatologies. J Clim 6 : 1301–1326

Stephens GL (1978) Radiation profiles in extended water clouds: 2. Parametrization schemes. J Atmos Sci 35 : 2123–2132

Warren SG, Hahn CJ, London J, Chervin RM, Jenne RL (1986) Global distribution of total cloud cover and cloud type amounts over land. DOE/ER/60085-H1, NCAR/TN-273 + STR, 29p

Wild M (1997) The heat balance of the Earth in GCM simulations of present and future climate. Zürcher Geograf Schr 68, Zürich, 188p (available from Geography Institute ETH, Winterthurerstr. 190, CH-8057 Zürich)

Wild M, Ohmura A, Gilgen H, Roeckner E (1995a) Validation of GCM simulated radiative fluxes using surface observations. J Clim 8 : 1309–1324

Wild M, Ohmura A, Gilgen H, Roeckner E (1995b) Regional climate simulation with a high resolution GCM: surface radiative fluxes. Clim Dyn 11 : 469–486

Wild M, Dümenil L, Schulz JP (1996) Regional climate simulation with a high resolution GCM: surface hydrology. Clim Dyn 12 : 755–774

Wild M, Ohmura A, Cubasch U (1997) GCM simulated surface energy fluxes in climate change experiments. J Clim 10 : 3093–3110.

Wild M, Liepert B (1998) Excessive transmission of solar radiation through the cloud-free atmosphere in GCMs. Geophysical Research Letters 25 : 2165–2168

Zdunkowski WG, Welch RM, Korb G (1980) An investigation of the structure of typical two stream methods for the calculation of solar fluxes and heating rates in clouds. Beitr Phys Atmos 53 : 147–166